

profiles then show a maximum at the temperature crossover point and drop to zero at the stratosphere base and at the bottom of the model atmosphere.

Figures 1 and 2 show  $T_A$  as a function of depth, and on an expanded scale the difference  $T_B - T_A$ , which is only on the order of 5 K for the Jupiter model and 10 K for the Saturn one. The wind maxima occur near the 1-bar pressure level and are about  $80 \text{ m sec}^{-1}$  for Jupiter and  $250 \text{ m sec}^{-1}$  for Saturn. These speeds are in rough agreement with observation. In particular, these results support the hypothesis of a relatively shallow dynamical regime on both planets, while offering an explanation for the differences between the two planets.

There has been no attempt in this construction to develop a self-consistent flow theory, but a feedback mechanism is suggested by the results. The pairs of temperature profiles ( $T_A$ ,  $T_B$ ) exhibit the magnitude of temperature differences which disequilibrium might cause. For their existence a downward flow would probably be required at location B, and a process analogous to conditional instability in the terrestrial atmosphere (7) is clearly possible. The initial motion would require energy to overcome unfavorable buoyancy, but a threshold would be passed after a certain displacement, beyond which buoyancy would be favorable to augment the motion.

The time scale for overturning would need to be on the same order as that for orthohydrogen-parahydrogen equilibration. The latter remains a pivotal unknown in these considerations. The equilibration time is very long at low temperatures in clean hydrogen gas (14), in excess of  $10^7$  seconds. The rate in the atmospheres of the outer planets is probably determined by the catalytic action of aerosols (7), whose abundance and composition are as yet unknown. This question needs work. Observations to date are consistent with thermal equilibrium (11, 15), but the uncertainties are large and horizontal resolution has been either nonexistent (whole-disk observations) or barely sufficient to resolve the scales of interest (Voyager infrared spectrometer observations). Disequilibrium could be confined to narrow updraft and downdraft areas.

*Note added in proof:* It now appears that the Voyager infrared data for Jupiter may indeed indicate significant disequilibrium (15).

PETER J. GIERASCH  
Center for Radiophysics and Space  
Research, Cornell University,  
Ithaca, New York 14853

#### References and Notes

1. R. A. Hanel, B. J. Conrath, L. W. Herath, V. G. Kunde, J. A. Pirraglia, *J. Geophys. Res.* **86**, 8705 (1981).
2. R. A. Hanel *et al.*, in *Saturn*, T. Gehrels, Ed., in preparation.
3. P. J. Gierasch, *Icarus* **29**, 445 (1976).
4. For example, D. D. Clayton, *Principles of Stellar Evolution and Nucleosynthesis* (McGraw-Hill, New York, 1968).
5. B. A. Smith *et al.*, *Science* **206**, 927 (1979).
6. B. A. Smith *et al.*, *ibid.* **215**, 504 (1982).
7. S. T. Massie and D. M. Hunten, *Icarus* **49**, 213 (1982).
8. For example, see J. R. Holton, *An Introduction to Dynamic Meteorology* (Academic Press, New York, 1979).
9. J. Tassoul, *The Theory of Rotating Stars* (Princeton Univ. Press, Princeton, N.J., 1978).
10. F. H. Busse, *Icarus* **29**, 255 (1976); \_\_\_\_\_ and C. R. Carrigan, *Science* **191**, 81 (1976).
11. W. H. Smith, *Icarus* **33**, 210 (1978).
12. For example, see G. H. Wannier, *Statistical Physics* (Wiley, New York, 1966).
13. R. A. Hanel *et al.*, *Science* **215**, 544 (1982).
14. A. Farkas, *Orthohydrogen, Parahydrogen, and Heavy Hydrogen* (University Press, Cambridge, 1935); see also Smith (11).
15. B. J. Conrath, private communication.
16. Supported in part by the NASA Voyager Project and the NASA Planetary Atmospheres Program. I thank B. Conrath, D. Hunten, and R. Thompson for helpful information.

23 April 1982; revised 9 July 1982

## Abyssal Water Carbon-14 Distribution and the Age of the World Oceans

**Abstract.** *The carbon-14 distribution in the abyssal waters of the world oceans indicates replacement times for Pacific, Indian, and Atlantic ocean deep waters (more than 1500 meters deep) of approximately 510, 250, and 275 years, respectively. The deep waters of the entire world ocean are replaced on average every 500 years.*

The Geochemical Ocean Sections Study (GEOSECS) program, initiated in 1971, was designed to inventory the chemical constituents in the world oceans. Such an inventory can be used for baseline studies of future chemical changes and for the investigation of large-scale oceanic transport and mixing processes. An important component of the GEOSECS program was the  $^{14}\text{C}$  sub-program. Twenty-two hundred samples were collected and extracted on board at 124 stations, of which 39 were in the Atlantic Ocean, 44 in the Pacific Ocean, and 41 in the Indian Ocean. These oceans were, respectively, sampled during the years 1972–1973, 1973–1974, and 1977–1978. The  $^{14}\text{C}$  activities ( $I$ ) of the samples were determined with an accuracy of 4 per mil at the University of

Miami (H.G.O.) and the University of Washington (M.S.). The laboratory measurements were completed in 1980, and we present here a comparison of the deepwater  $^{14}\text{C}$  concentrations of the three oceans.

The  $^{14}\text{C}$  distribution of the carbon species in the deep ocean is influenced by many processes. Bottom-water formation in the North Atlantic and the Weddell Sea provides a direct input of surface-water  $^{14}\text{C}$ . Additional input of  $^{14}\text{C}$  to the deep sea can occur by transport along isopycnal surfaces and by vertical mixing in the main oceanic thermocline. An addition of  $\text{CO}_2$  and  $^{14}\text{C}$  is provided by the dissolution of carbonate skeletons and the oxidation of organic materials from sinking particles. Mixing between laterally moving water masses and up-

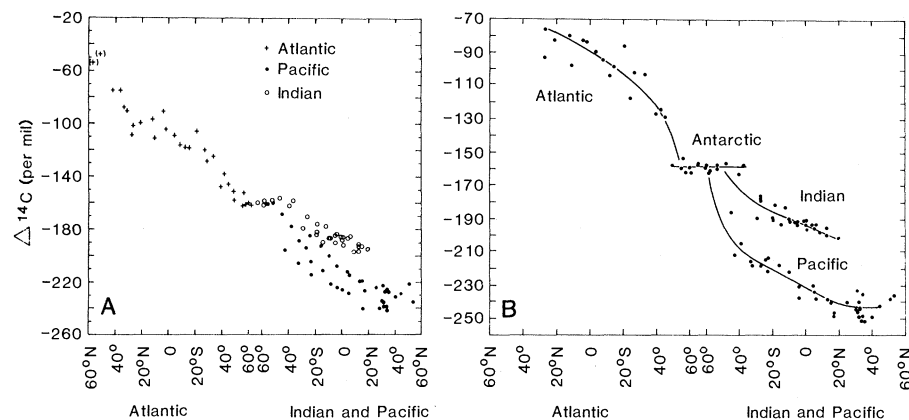


Fig. 1. (A) Average  $\Delta^{14}\text{C}$  values of waters below a depth of 1500 m for Atlantic, Pacific, and Indian ocean GEOSECS stations. The bracketed points near  $60^\circ\text{N}$  in the Atlantic are influenced by nuclear bomb  $^{14}\text{C}$ . The southern boundary of the circumpolar current is taken at  $65^\circ\text{S}$ . Circumpolar waters, south of  $50^\circ\text{S}$ , have nearly uniform  $\Delta^{14}\text{C}$  values. (B) The  $\Delta^{14}\text{C}$  values of the cores of North Atlantic, Pacific, and Indian ocean deep waters. The oldest waters are encountered near  $40^\circ\text{N}$  in the Pacific Ocean.

welling of  $^{14}\text{C}$ -deficient water in the equatorial regions and along continental margins also influence the oceanic  $^{14}\text{C}$  distribution. Whereas other oceanographic markers such as salinity are conservative properties,  $^{14}\text{C}$  adds a measure of time because it decays at a fixed rate of 1 percent every 83 years.

The exchange of waters between the major oceans takes place through the Antarctic circumpolar waters. The  $^{14}\text{C}$  content of the deep circumpolar water (> 1500 m deep) is remarkably uniform. The average  $\Delta^{14}\text{C}$  value of 155 samples collected at 16 stations (all south of  $49.5^\circ\text{S}$ ) is  $-158.1$  per mil, with a standard deviation of 6.0 per mil. The measuring precision of each  $^{14}\text{C}$  determination is 3.5 per mil.

The deepwater  $^{14}\text{C}$  distributions in the Atlantic, Pacific, and Indian oceans are shown in Fig. 1. The latitudes of the stations are plotted for each ocean along the abscissa. The common point of exchange between the Atlantic, Pacific, and Indian oceans is the circumpolar system with its southern boundary at  $65^\circ\text{S}$ .

The  $\Delta^{14}\text{C}$  values given in Fig. 1 have not yet been influenced by nuclear bomb  $^{14}\text{C}$ , except for the North Atlantic where tritium measurements show the sinking of considerable amounts of modern water (2). The tabulation of the individual  $\Delta^{14}\text{C}$  data is given in (3).

The North Atlantic deep water, with its most recent atmospheric  $^{14}\text{C}$  uptake, has the highest  $^{14}\text{C}$  concentration (Fig. 1A). The circumpolar water has a uniform  $^{14}\text{C}$  concentration which defines the  $^{14}\text{C}$  values of the southern borders (about  $50^\circ\text{S}$ ) of the Atlantic, Pacific, and Indian oceans. Both the Indian and Pacific oceans have lower  $^{14}\text{C}$  concentrations than the circumpolar system, and the Pacific Ocean has the lowest  $^{14}\text{C}$  concentration of all the world's oceans.

These trends in the  $^{14}\text{C}$  characteristics of the world oceans are even more apparent in Fig. 1B, which is a plot of the

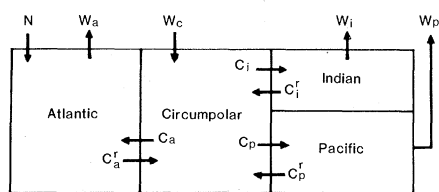


Fig. 2. Box model of the deep ocean (> 1500 m). The rates of bottom-water formation are  $N$  and  $W_c$ ; the rates of upwelling are  $W_a$ ,  $W_p$ , and  $W_i$ ; and the mass transport rates between the circumpolar ocean and the other oceans are  $C_a$ ,  $C_a^r$ ,  $C_p$ ,  $C_p^r$ ,  $C_i$ , and  $C_i^r$ .

$\Delta^{14}\text{C}$  values of the "core" of the deep-water mass of each ocean versus latitude. In the Atlantic this core water is at the  $^{14}\text{C}$  maximum of North Atlantic Deep Water (NADW), whereas in the Pacific and Indian oceans the core water is chosen to coincide with the  $^{14}\text{C}$  minimum ( $\sim 2500$  m).

The range in preanthropogenic  $\Delta^{14}\text{C}$  values measured in the deep sea shows a high of  $-75$  per mil in the North Atlantic (4) and a low of  $-245$  per mil in the North Pacific (Fig. 1B). If only radioactive decay caused this  $^{14}\text{C}$  decrease, it would take 1680 years. However, the deep oceans are not a completely closed system, and the  $^{14}\text{C}$  age does not necessarily represent the real age of the ocean water. Mixing with surrounding water masses tends to change  $\Delta^{14}\text{C}$  values. Biological transport adds  $^{14}\text{C}$  but to a limited extent (5).

Despite these complications, it is possible to derive the transport rates of deep water into each ocean basin and estimate the residence time of the deep sea from the  $\Delta^{14}\text{C}$  values measured during the GEOSECS program. A box model is used to represent the deepwater circulation of the world ocean (Fig. 2). The model has two sites of deepwater formation, one in the North Atlantic ( $N$ ) and one in the circumpolar ocean south of  $50^\circ\text{S}$ . Upwelling balances the net input of deep water to each ocean basin. The homogeneous  $^{14}\text{C}$  concentrations in the

circumpolar ocean provide the boundary condition ( $\Delta^{14}\text{C} = -158$  per mil) for all waters crossing the  $50^\circ\text{S}$  boundary in both directions. Because the measured  $^{14}\text{C}$  activity varies with depth (except for the circumpolar ocean) (5), we assume that the water upwelling (across the 1500-m level) has a  $^{14}\text{C}$  activity equal to the average  $^{14}\text{C}$  activity measured at 1500 m north of  $50^\circ\text{S}$ . Thus the box model provides for some of the observed heterogeneity in the  $^{14}\text{C}$  distribution by not treating the ocean basins as well-mixed reservoirs. The mass and  $^{14}\text{C}$  balances for each ocean are presented in Table 1.

The situation is simplest for the Indian and Pacific oceans where there are no significant northern deepwater formation sites. Thus the deep waters of these oceans are replaced solely by water from the circumpolar ocean. The input of  $^{14}\text{C}$  from the circumpolar ocean balances the loss of  $^{14}\text{C}$  resulting from decay, upwelling, and deepwater return flow to the circumpolar ocean.

For the Indian and Pacific oceans, the mass and  $^{14}\text{C}$  balances can be used to determine the net transport rates from the circumpolar ocean (that is,  $C_i - C_i^r$ , see Fig. 2) which are balanced by basin-wide upwelling. For the Indian Ocean the calculated net transport from the circumpolar ocean is 20 sverdrups ( $1 \text{ Sv} = 10^6 \text{ m}^3 \text{ sec}^{-1}$ ). This transport rate corresponds to an abyssal water replacement time of 250 years and an average rate of upwelling of  $10 \text{ m year}^{-1}$ . For the Pacific Ocean the calculated net transport from the circumpolar ocean is 25 Sv, resulting in a deepwater replacement time of 510 years and an upwelling rate of  $5 \text{ m year}^{-1}$ . These transport rates from the circumpolar ocean are in good agreement with Warren's geostrophic calculations of the transport rates for the Indian (16 Sv) and Pacific (24 Sv) oceans (6).

The calculation of deepwater residence times for the Atlantic Ocean is

Table 1. Mass and  $^{14}\text{C}$  balances for the world oceans. The deepwater  $\Delta^{14}\text{C}$  values have been corrected for biological  $^{14}\text{C}$  addition. Because of this correction, a constant total  $\text{CO}_2$  value is used in the  $^{14}\text{C}$  balance equations. The remaining terms in the  $^{14}\text{C}$  balance equations are the  $^{14}\text{C}$  decay constant  $\lambda$  and  $^{14}\text{C}_w$ , which is the  $^{14}\text{C}$  activity of the deep water forming within the circumpolar ocean. As an example of the nomenclature,  $C_a$  ( $-158$ ) is the mass transport  $C_a$  (in cubic meters per second) multiplied by the  $^{14}\text{C}$  activity ( $1 - 158/1000$ ). The other parameters are explained in the text and the legend to Fig. 2.

| Ocean       | Volume (north of $50^\circ\text{S}$ ) ( $10^{18} \text{ m}^3$ ) | Average deep water (>1500 m) $\Delta^{14}\text{C}$ (per mil) | Average $\Delta^{14}\text{C}$ (per mil) at 1500 m | Mass balance                                    | $^{14}\text{C}$ balance (per mil)   |
|-------------|---|--|---|---|---|
| Atlantic    | 0.18  | -118   | -100  | $N + C_a = C_a^r + W_a$                         | $N(-75) + C_a(-158) = C_a^r(-158) + W_a(-100) + V_a\lambda(-118)$                           |
| Circumpolar | 0.11 (south of $50^\circ\text{S}$ )                             | -158   | -158  | $W_c = C_a - C_a^r + C_p - C_p^r + C_i - C_i^r$ | $W_c(^{14}\text{C}_w) = [C_a - C_a^r + C_p - C_p^r + C_i - C_i^r](-158) + V_c\lambda(-158)$ |
| Indian      | 0.16  | -184   | -181  | $C_i = C_i^r + W_i$                             | $C_i(-158) = C_i^r(-158) + W_i(-181) + V_i\lambda(-184)$                                    |
| Pacific     | 0.41  | -217   | -207  | $C_p = C_p^r + W_p$                             | $C_p(-158) = C_p^r(-158) + W_p(-207) + V_p\lambda(-217)$                                    |

more complicated because there are two sources of deep water: one originating within the the circumpolar ocean—that is, Antarctic Bottom Water (AABW)—and one in the north (NADW), each with distinctly different  $^{14}\text{C}$  concentrations. The preanthropogenic  $\Delta^{14}\text{C}$  value of NADW source water is estimated at  $-75 \pm 5$  per mil (4, 7), whereas the deep water entering from the circumpolar ocean has a  $\Delta^{14}\text{C}$  value of  $-158$  per mil. The mass balance for the Atlantic Ocean (Table 1) is described in terms of four transport terms ( $N$ ,  $C_a$ ,  $C_a^r$ , and  $W_a$ ). We assume the northern source input to be twice that of the southern source ( $N = 2C_a$ ), as indicated by Broecker (7), on the basis of the  $\text{NO}_3^-$ ,  $\text{O}_2$ , and  $\text{SiO}_2$  characteristics of the deep water of the Atlantic Ocean.

Estimating the four transport terms for the deep water of the Atlantic Ocean requires that one of these be set. Earlier estimates of the NADW transport, based on either  $^{14}\text{C}$  distribution or geostrophic calculations, range from 9 to 20 Sv (4, 7–9). Here we have assigned a median value of 14 Sv for the NADW transport. Because  $N = 2C_a$ , the southern deepwater source is then fixed at 7 Sv, in good agreement with earlier geostrophic and  $^{14}\text{C}$  calculations of AABW transport (4, 9).

If we solve the mass and  $^{14}\text{C}$  balances for  $N = 14$  Sv, we obtain  $C_a = 7$  Sv,  $C_a^r = 11$  Sv, and  $W_a = 10$  Sv (10). These transport calculations indicate a deepwater residence time for the Atlantic Ocean of 275 years, corresponding to a basin-wide upwelling rate of  $4 \text{ m year}^{-1}$ . There is also a net southward flow of deep water from the Atlantic to the circumpolar ocean ( $C_a^r > C_a$ ) of 4 Sv, in contrast to the net northward flow from the circumpolar to the Indian and Pacific oceans.

Our transport calculations indicate that approximately 41 Sv of bottom water ( $> 1500$  m) must be forming within the entire circumpolar ocean, resulting in an 85-year residence time for the deep circumpolar ocean. The  $^{14}\text{C}$  balance in the circumpolar ocean (Table 1) implies that this “new” deep water has  $\Delta^{14}\text{C} = -149$  per mil, in good agreement with earlier estimates of  $-148$  to  $-152$  per mil (11).

Deep-sea residence times are important for climate modeling and nuclear waste disposal. Whereas some parcels of water may have been isotopically isolated from the surface for up to 1700 years, the average replacement time of the abyssal waters in the oceans is much shorter. A parcel of bottom water formed near Antarctica will surface

again after an average of 595 or 335 years, depending on its Pacific or Indian ocean choice. A parcel of deep water will reside in the Atlantic about 275 years. The overall replacement time for the entire deep ocean (which is influenced most by the residence time of the deep Pacific Ocean) averages about 500 years when the realities of abyssal circulation and  $^{14}\text{C}$  atmosphere-ocean exchange are taken into account.

MINZE STUIVER

PAUL D. QUAY

Quaternary Research Center,  
University of Washington,  
Seattle 98195

H. G. OSTLUND

Tritium Laboratory, University of  
Miami, Miami, Florida 33149

#### References and Notes

1. The  $^{14}\text{C}$  activity of the sample ( $A_s$ ) was compared to the age-corrected  $^{14}\text{C}$  activity of the National Bureau of Standards (NBS) oxalic acid standard ( $A_{ox} = 0.95$  NBS activity), after appropriate normalization to a  $\delta^{13}\text{C}$  value of  $-25$  per mil for the samples and  $-19$  per mil for the standard. The results are expressed as  $\Delta^{14}\text{C} = (A_s/A_{ox} - 1)1000$  per mil. Because the comparison of  $A_s$  and  $A_{ox}$  is made for identical amounts of carbon, the quantity  $(1 + \Delta^{14}\text{C}/1000)$  is a measure of the specific sample activity. The  $^{14}\text{C}/\text{C}$  ratio of the oxalic acid standard is known [M. Stuiver, *Radiocarbon* 22, 964 (1980)], and the absolute quantity ( $\Sigma^{14}\text{C}$ ) of  $^{14}\text{C}$  in a sample is given by

$$\Sigma^{14}\text{C} = 1.176 \times 10^{-12}(1 + \Delta^{14}\text{C}/1000)\Sigma\text{CO}_2$$

- where both  $\Sigma^{14}\text{C}$  and  $\Sigma\text{CO}_2$  are expressed in identical units (for instance, micromoles per kilogram of seawater). The technical details of the measurements and calculation, and also the discussion of the age correction of the oxalic acid standard, are given in M. Stuiver, S. W. Robinson, H. G. Ostlund, H. G. Dorsey, *Earth Planet. Sci. Lett.* 23, 65 (1974); M. Stuiver and S. W. Robinson, *ibid.*, p. 87.
2. H. G. Ostlund, H. G. Dorsey, C. G. Rooth, *Earth Planet. Sci. Lett.* 23, 69 (1974).
3. M. Stuiver and H. G. Ostlund, *Radiocarbon* 22, 1 (1980); H. G. Ostlund and M. Stuiver, *ibid.*, p. 25; M. Stuiver and H. G. Ostlund, *ibid.*, in press.
4. M. Stuiver, *Earth Planet. Sci. Lett.* 32, 322 (1976).
5. ———, H. G. Ostlund, T. A. McConnaughey, in *Carbon Cycle Modelling: Scope*, B. Bolin, Ed. (Wiley, New York, 1981), vol. 16, p. 201.
6. B. A. Warren, *Deep-Sea Res.* 28A, 759 (1981); *ibid.* 20, 9 (1973).
7. W. S. Broecker, *J. Geophys. Res.* 84, 3218 (1979).
8. H. Stommel and A. B. Arons, *Deep-Sea Res.* 6, 217 (1960).
9. W. R. Wright, *ibid.* 17, 367 (1970).
10. Extreme ranges of the model estimates can be obtained if one combines the limits of NADW transport estimates with the maximum errors in the NADW source  $\Delta^{14}\text{C}$  value. A range of  $N = 9$  to 20 Sv would result in a range of  $C_a = 4.5$  to 10 Sv,  $C_a^r = 10$  to 13 Sv, and  $W_a = 2$  to 12 Sv. The corresponding range for Atlantic deepwater replacement time is 190 to 425 years. The upper limit increases to 480 years for  $N = 3C_a$ .
11. R. F. Weiss, H. G. Ostlund, H. Craig, *Deep-Sea Res.* 26, 1093 (1979).
12. We thank P. M. Grootes, H. Bryden, and W. S. Broecker who made valuable suggestions for the improvement of the manuscript and T. A. McConnaughey who assisted in the calculations of the  $\Delta^{14}\text{C}$  averages. This work was supported by National Science Foundation grant OCE77-23765 and Department of Energy contract 19X-43303-C to the University of Washington and National Science Foundation grant OCE77-24039 to the University of Miami.

7 June 1982; revised 29 October 1982

## Tumor Suppression with a Combination of $\alpha$ -Difluoromethyl Ornithine and Interferon

Abstract.  $\alpha$ -Difluoromethyl ornithine and mouse type 1 interferon, when administered simultaneously, were highly toxic to B16 melanoma cells in culture. Oral administration of  $\alpha$ -difluoromethyl ornithine suppressed B16 melanoma development in mice 85 percent whereas interferon given subcutaneously inhibited tumor growth only 24 percent. Total or near total suppression of tumor growth was observed in mice receiving both treatments.

It is thought that the naturally occurring polyamines putrescine, spermidine, and spermine play an important role in cell growth processes (1). Studies with  $\alpha$ -difluoromethyl ornithine (DFMO), an irreversible inhibitor (2) of ornithine decarboxylase, the first step in polyamine biosynthesis, have demonstrated that DFMO retards the growth of a number of tumor cell lines both in vitro and in vivo (3, 4). Interferons are a group of glycoproteins with antiviral, anticellular, antitumor, and immunoregulatory activities (5, 6). It was recently reported that the decrease in the growth rate of cells treated with interferon is accompanied by a rapid loss in the activities of the polyamine biosynthetic enzymes ornithine decarboxylase and S-adenosylmethionine decarboxylase (7). Interferon re-

tards a number of animal tumors (8) and some malignancies in man (9). DFMO treatment of mice bearing B16 melanomas inhibits tumor growth about 80 percent. These findings prompted us to examine the effects of DFMO and interferon, both separately and in combination, on the growth of B16 melanoma cells in vitro and in vivo. We found that the combination of the two agents markedly suppresses the tumor.

Melanoma cells (B16, line F<sub>1</sub>) were grown as monolayers at 37°C in minimal essential medium supplemented with 10 percent fetal calf serum and antibiotics in an atmosphere containing 5 percent  $\text{CO}_2$ . Treatment with DFMO (2.5 mM) or mouse fibroblast interferon (type 1, 100 U/ml) inhibited cell growth 67 and 40 percent, respectively, after 5 days. How-